Eur Biophys J (2009) 38:569–576
DOI 10.1007/s00249-009-0408-2

ORIGINAL PAPER

# Role of intracellular domains in the function of the herg potassium channel

**Moza Al-Owais · Kate Bracey · Dennis Wray**

Received: 27 November 2008 / Revised: 24 December 2008 / Accepted: 2 January 2009 / Published online: 27 January 2009


**Abstract** The functional role of the large intracellular regions (which include the cyclic nucleotide binding domain, cNBD, and the Per-Arnt-Sim domain, PAS) in the herg channel is not well understood. We have studied possible interactions of the cNBD with other parts of the channel protein using lysine mutations to disrupt such interactions. Some lysine mutations caused significant right shifts in the voltage dependence of inactivation; almost all the mutants caused speeding up of deactivation time course. In a homology model of the cNBD, lysine mutations that affected both inactivation and deactivation lie in a hydrophobic band on the surface of the structure of this domain. Some known mutations in the Long QT Syndrome type 2, with effects on deactivation, are located at residues close to hydrophobic bands on the cNBD and the PAS domains. Such bands of residues in these intracellular domains may play an important part in channel function.

**Keywords** Human ether-a-go-go-related gene · Herg · Cyclic nucleotide binding domain · Potassium channel · Electrophysiology

## Introduction

The human ether-a-go-go related gene (herg) encodes the $K_v11.1$ potassium channel, which plays a crucial role in the $I_{kr}$ current component of the cardiac action potential (Sanguinetti et al. 1995; Tseng 2001). Many mutations in herg have been found in inherited cardiac disorders characterised by prolongation of the QT interval, leading to susceptibility to arrhythmias and even sudden death (Bracey and Wray 2006). In herg, the disorder is referred to as Long QT Syndrome type 2 (LQT2) (Finlayson et al. 2004). Partial or complete loss of function introduced by the mutations inhibits the normal repolarisation of the cardiac action potential via $I_{kr}$ suppression or alteration, leading to lengthening of the ventricular action potential duration and hence a long QT interval in the electrocardiogram (Lehmann-Horn and Jurkat-Rott 1999). Over a hundred mutations of herg have been linked to LQT2 and many have been characterised electrophysiologically and by their biosynthetic processing (www.pc4.fsm.it:81/cardmoc/index.html).

Clearly, a greater understanding of the structure–function relationship of the herg channel itself will help in understanding the effect of these mutations at the protein level. The herg channel itself is a tetramer, with each subunit having six transmembrane regions (S1–S6), a feature held in common with other members of the very large family of voltage-activated potassium channels (Warmke and Ganetzky 1994; Vandenberg et al. 2004). The membrane-spanning section of the channel is vital for its voltage-dependent function, with the S4 region functioning as the voltage sensor (Yusaf et al. 1996; Ferrer et al. 2006).

The herg channel belongs to a smaller family of eight members each characterised by the long intracellular amino- and carboxy-terminal regions of their subunits. These regions include a Per-Arnt-Sim (PAS) domain in the N terminal region. PAS domains were originally identified in several proteins in procharyotes and lower eukaryotes and appear to be involved in protein–protein interactions; some mammalian PAS domain proteins are involved in circadian rhythms (Wu and Wang 2004; Zhulin et al. 1997). The herg channel also has a cyclic nucleotide binding domain (cNBD) in the C terminal region (Morais Cabral

M. Al-Owais · K. Bracey · D. Wray (✉)
Faculty of Biological Sciences,
University of Leeds, Leeds LS2 9JT, UK
e-mail: d.wray@leeds.ac.uk

et al. 1998). For the homologous HCN channel (hyperpolarisation and cyclic nucleotide-activated channel) (Zagotta et al. 2003), the cNBD hangs as a tetramer below the membrane, and it is reasonable to assume a similar structure for the herg channel, with the cNBD tetramer surrounded by the other intracellular regions such as the PAS domain. Thus it is likely that the surface regions of the cNBD domain interact with other intracellular regions of the channel protein. To study this, we have made lysine mutations in residues of the cNBD that are predicted to lie on the surface of the domain in a homology model for the structure of this domain. Such mutations can disrupt domain–domain (or subunit–subunit) interaction at hydrophobic regions and so may be useful in identifying regions of structural and functional interaction (Sine et al. 2002). Lysine mutations have, for example, previously been used to characterise surfaces involved in channel–toxin interactions (Li-Smerina and Swartza 2001). Such an approach has not previously been carried out for the cNBD of the herg channel. For comparison purposes under the same experimental conditions, besides studying lysine mutations, we have also chosen for study some known LQT2 mutations in the PAS and cNBD domains. Our overall aim is to investigate possible interacting surfaces of these domains, which may also shed light on possible mechanisms for the functional effects of some of the LQT2 mutations at surface residues of these domains.

## Materials and methods

Mutations were introduced into wild-type herg (provided in pSP64, a kind gift from Professor M. Sanguinetti, University of Utah) by site-directed mutagenesis using QuikChange site directed mutagenesis (Stratagene, UK) according to the manufacturer's instructions. Before use in expression experiments, the constructs were verified by DNA sequence analyses. Plasmids containing the mutated herg genes were linearised with *Eco*RI, and RNA prepared using SP6 Megascribe (Ambion, Oxfordshire, UK) according to the manufacturer's instructions.

*Xenopus laevis* toads were anaesthetized by immersion in 0.1% ethyl 3-aminobenzoate methanesulfonate for 1 h. Ovarian lobes were then digested with 2 mg $ml^{-1}$ type 1A collagenase (Sigma) in $Ca^{2+}$-free Ringers solution for 60 min to remove follicle cells. Stages IV and V oocytes were injected with herg RNA (5 ng), then incubated in Barth's solution (88 mM NaCl, 1 mM KCl, 0.4 mM $CaCl_2$, 0.33 mM $Ca(NO_3)_2$, 0.82 mM $MgSO_4$, 2.4 mM $NaHCO_3$, 7.25 mM Tris–HCl, pH 7.6) supplemented with benzylpenicillin (10 μg $ml^{-1}$) and streptomycin sulphate (10 μg $ml^{-1}$) at 19.4°C for 2 days.

Oocytes were bathed in Ringer's solution containing 115 mM NaCl, 2 mM KCl, 1.8 mM $CaCl_2$, 10 mM HEPES, pH 7.2. Currents were recorded at room temperature (21–24°C) using standard two-microelectrode voltage-clamp techniques. Glass microelectrodes were filled with 3 M KCl (resistances of 0.5–1.5 MΩ). Oocytes were voltage clamped with a GeneClamp 500 amplifier (Axon Instruments, Foster City, CA). Voltage commands were generated using Signal CED software and a 1401plus CED interface (Cambridge Electronic Design, Cambridge, UK).

Tail current time course was recorded using a 1 s prepulse to +40 mV and then a step to the test potential (Fig. 1a); the time course was fit with a double exponential function. The voltage dependence of activation was determined from peak tail currents measured at −40 mV following 1 s test depolarizations (Fig. 2a). The peak tail current, $I$, was fit with a Boltzmann function as follows, $I = I_{max}/(1 + \exp((V_{0.5} - V)/k))$ where $I_{max}$ is the maximum current, $V$ is the test potential, $V_{0.5}$ is the potential for half-maximal activation and $k$ is the slope factor. The voltage dependence of herg inactivation was determined using a three-pulse voltage protocol (Numaguchi et al. 2000) (Fig. 3a); a prepulse to +60 mV was applied for 3 s to activate and then fully inactivate the channels, followed by a 20 ms step to various test potentials allowing recovery from inactivation without appreciable deactivation, and then the peak of the inactivating current was measured during a final step to +30 mV. A Boltzmann function was again fitted to the peak currents. The assumption of lack of appreciable deactivation during the short 20 ms activating test pulse used in these experiments holds true for herg wild-type channels. However, for those of the mutants with faster deactivation than wild type, the voltage dependence of the deactivation time course may somewhat distort the observed steady-state inactivation curve, but we have not attempted to correct for this factor. For each experiment with injected oocytes, a negative control consisting of uninjected oocytes was always carried out, recorded under the same conditions and protocols. The negative control current amplitude corresponding to peak tail or peak inactivating currents was always negligible compared with the herg peak currents, and so no leak subtraction was carried out.

Data were analysed using Origin (Northampton, MA) and Excel (Microsoft, UK) software. Data are presented as mean ± standard error. Statistical comparisons were made using the Student's $t$ test, with $P < 0.05$ taken as statistically significant.

## Results

We have made lysine mutations of residues that are predicted to lie on the surface regions of the cNBD, in order to investigate possible interactions with other protein regions of the channel, on the basis that lysine mutations

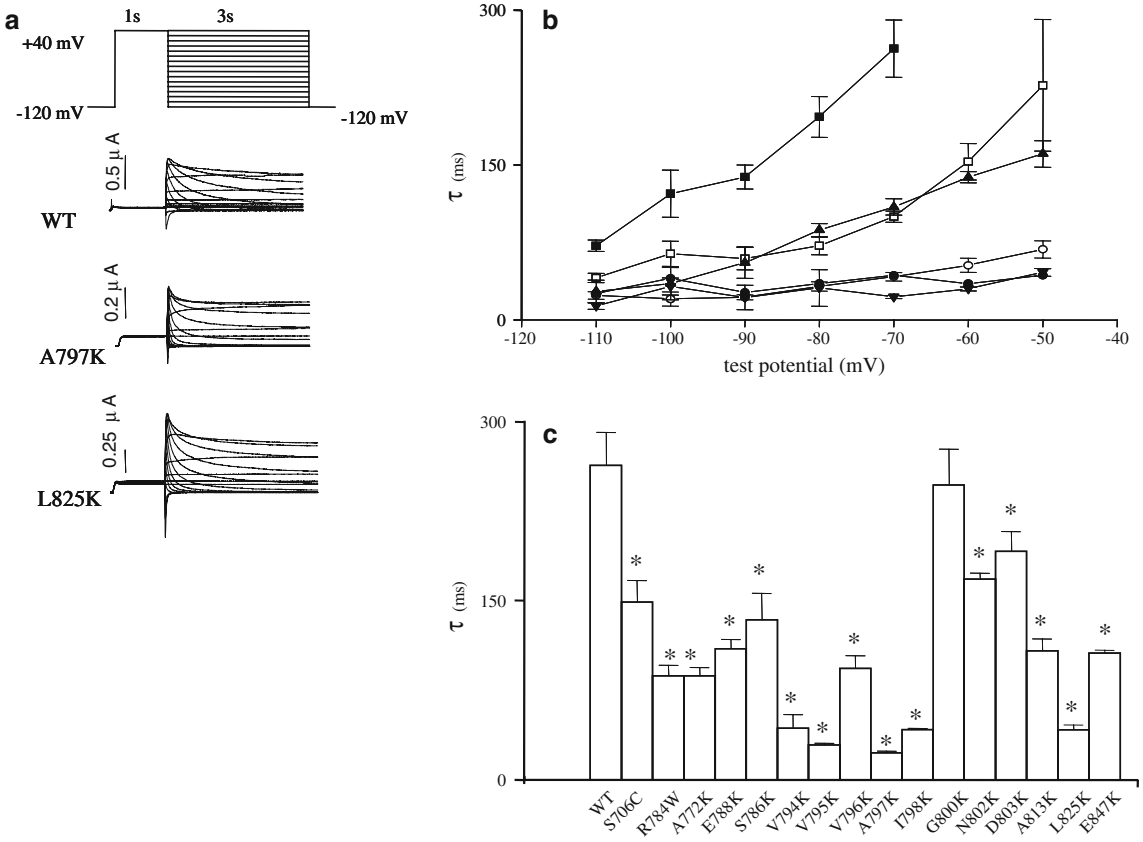


**Fig. 1** Deactivation time course of herg mutants in the cNBD. **a** The protocol used and examples of currents are shown. **b** The mean time constant, $\tau$, of the fast component of current deactivation is shown plotted against test potential for herg (*filled square*) WT, E788K (*filled triangle*), V795K (*filled circle*), A797K (*filled invertedtriangle*), E847K (*open square*), L825K (*open circle*). **c** The mean time constant for the fast component of deactivation, $\tau$, measured at −70 mV, is shown for the cNBD mutations indicated ($n$ = 6–22 cells, $^*P < 0.05$)

can disrupt interactions between protein domains. We chose such mutations on the surface of this domain on the basis of our homology model for the herg cNBD region (including the linker to S6) discussed further below. We have also tested some known selected LQT2 mutations for comparison under the same laboratory conditions.

To assess the functional consequences of each mutation, we performed two-electrode voltage-clamp experiments. We first examined the time constants for deactivation of the lysine mutants, using the protocol shown in Fig. 1a, which also shows example current traces. The time constants were determined by fitting tail currents to two-component exponential functions. Examples of the fast time constant as a function of test potential are shown for wild type and mutant channels (Fig. 1b), showing faster deactivation for the mutants in comparison to the wild type. The fast time constant measured at −70 mV test potential is shown in Fig. 1c for all the mutants investigated. It can be seen that, for all lysine mutations except one, there was significantly faster deactivation than wild type for the fast time constant. The time constants for the slow components were also faster for the lysine mutants than for the wild-type channels, but there was more scatter in the data (not shown). For comparison, we also studied LQT2 mutations in the cNBD region, R784W and S706C (Fig. 1c), which also gave faster deactivation time course than wild type, in agreement with Yang et al. 2002 and Kobori et al. 2004.

Next, we examined the voltage dependence of steady-state activation for the lysine mutants in cNBD. The protocol used and example traces are shown in Fig. 2a, and examples of steady-state activation curves are depicted in Fig. 2b. The lysine mutations did not have any affect on steady-state activation, and indeed the Boltzmann $V_{0.5}$ and $k$ values did not differ significantly from wild-type values (Table 1). The LQT2 mutation R784W also showed no effect on activation (the S706C mutant was not examined for activation).

Steady-state inactivation was studied using the protocol shown in Fig. 3a. Examples of steady-state inactivation curves are shown in Fig. 3b, where it can be seen that there were shifts to the right for the lysine mutations depicted in the figure. Figure 3c shows the Boltzmann $V_{0.5}$ values for all the lysine mutations studied here, indicating that lysine substitution caused marked right shifts for 9 out of 14

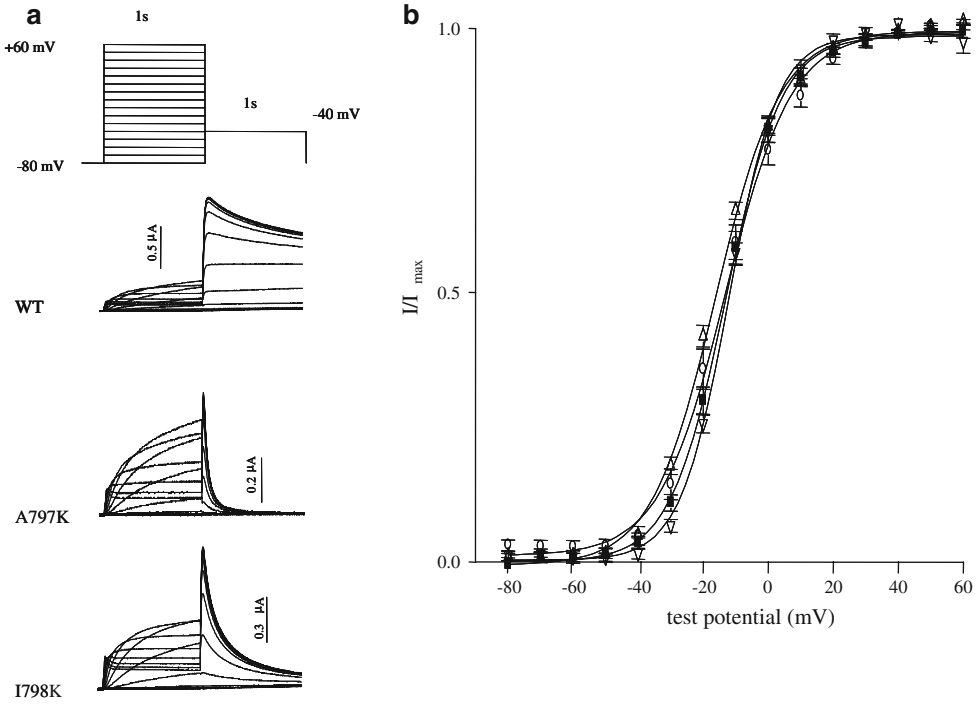


**Fig. 2** Voltage dependence of steady-state activation for mutants in the cNBD. **a** The pulse protocol and examples of currents are shown. **b** The mean normalized tail current peak amplitude, $I/I_{max}$, is shown plotted against test potential for WT (*filled square*), V794K (*open circle*), I798K (*open triangle*), A797K (*open invertedtriangle*). Numbers of cells used are given in Table 1

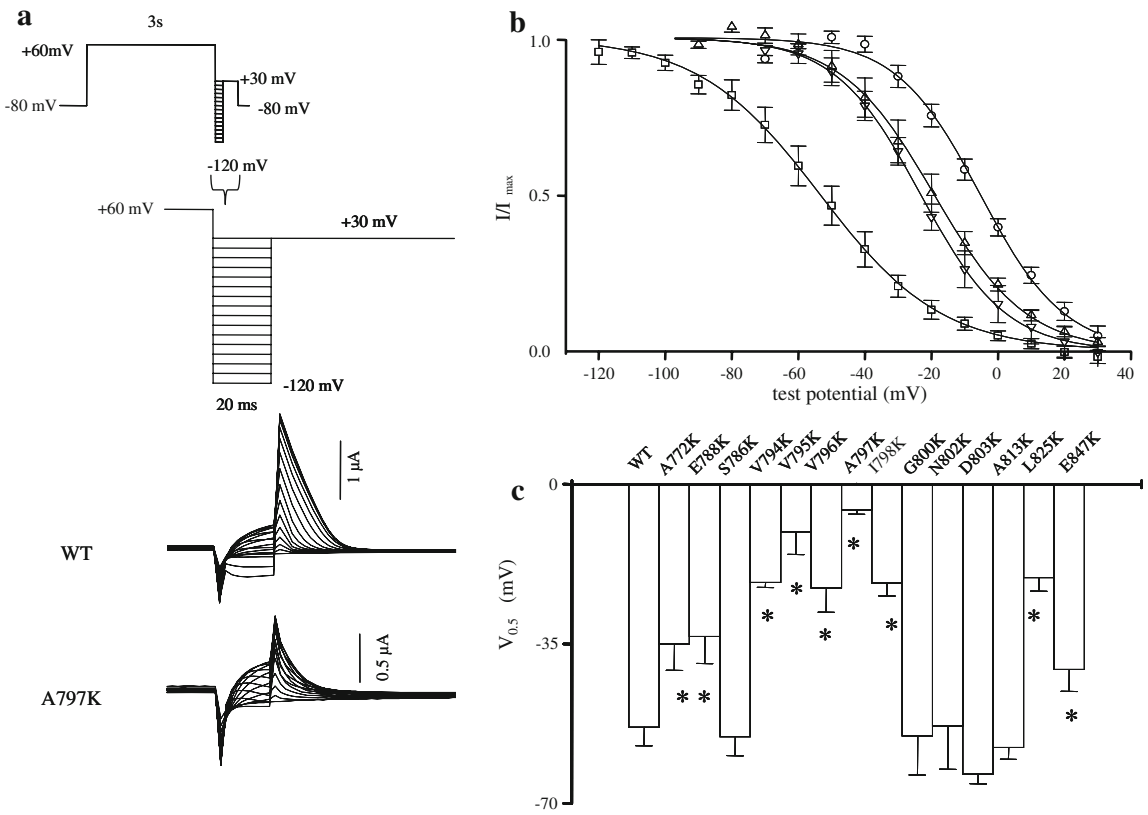


**Fig. 3** Voltage dependence of steady-state inactivation for mutants in the cNBD. **a** The *upper* panel shows the voltage pulse protocol used with an expanded view below, along with example currents. **b** The mean normalized tail current peak amplitude, $I/I_{max}$, is shown plotted against test potential for WT (*open square*), A797K (*open circle*), L825K (*open triangle*), I798K (*open invertedtriangle*). **c** The mean value of the Boltzmann parameter for inactivation, $V_{0.5,}$ is shown for the cNBD mutations indicated ($n$ = 6–14 cells, $^*P < 0.05$)

**Table 1** Boltzmann parameters for steady-state activation

| Mutant | $V_{0.5}$ (mV) | $k$ (mV) | $n$ |
|---|---|---|---|
| WT | −13.1 ± 0.6 | 8.6 ± 0.2 | 22 |
| A772K | −10.7 ± 2.1 | 8.5 ± 1.4 | 6 |
| R784W | −11.8 ± 2.9 | 6.1 ± 1.0 | 5 |
| S786K | −15.2 ± 0.9 | 8.1 ± 0.5 | 6 |
| E788K | −16.1 ± 2.3 | 9.0 ± 0.9 | 6 |
| V794K | −13.2 ± 1.3 | 10.0 ± 0.5 | 6 |
| V795K | −8.3 ± 2.1 | 8.7 ± 0.7 | 6 |
| V796K | −13.1 ± 1.8 | 11.9 ± 1.6 | 10 |
| A797K | −11.9 ± 0.7 | 7.6 ± 0.4 | 6 |
| I798K | −16.3 ± 0.9 | 9.7 ± 0.5 | 6 |
| N802K | −16.2 ± 1.1 | 9.4 ± 0.6 | 7 |
| D803K | −12.1 ± 2.0 | 7.0 ± 0.1 | 6 |
| A813K | −10.7 ± 2.3 | 8.6 ± 1.4 | 6 |
| L825K | −8.1 ± 3.7 | 11.9 ± 1.9 | 5 |
| E847K | −12.4 ± 1.4 | 7.6 ± 0.6 | 7 |

Values of $V_{0.5}$ and $k$ are shown for WT and mutant channels, along with the number of cells used for each, $n$. There were no significant differences for parameters between wild type and mutants

mutants. The slope factor, $k$, was not significantly altered by any of the lysine mutant channels (data not shown). It is interesting to compare the magnitudes of the shifts in steady-state inactivation, $V_{0.5}$, with the effects on deactivation time constant, $\tau$. It can be seen (Fig. 4b) that mutations which gave large effects on $V_{0.5}$ also tended to give large effects on $\tau$. However, some of this effect on $V_{0.5}$ may be quantitatively distorted by the methodology of the protocol used to obtain the inactivation parameters (see "Materials and methods").

Our homology model for the herg cNBD region (including the linker to S6) was constructed using Swiss-Model (http://swissmodel.expasy.org/SWISS-MODEL.html) by homology to the available crystal structure for the cNBD in the HCN2 channel (Zagotta et al. 2003), with 46% similarity between amino acids in the two structures. The positions of the residues studied here on the surface of the herg cNBD homology model are shown in Fig. 4a, indicating in red the residues with significant effect on both inactivation and deactivation. It is very striking that most residues that affected both these parameters lie in a band across the side of the cNBD tetramer, mostly corresponding to hydrophobic and conserved residues. This is suggestive of a region of interaction of this surface with other domains of the herg channel. The location of the LQT2 mutation R784W on the surface of the cNBD domain is also shown in Fig. 4a (the other LQT2 mutation studied here, S706C, lies more deeply within the cNBD structure).

For completeness and for comparison purposes in the same laboratory under the same experimental conditions, we also studied some LQT2 mutations located in the PAS domain, which is another important intracellular domain of the herg channel. Figure 5a shows the effect of the LQT2 mutations in the PAS domain on deactivation time constant. Again, it can be seen that there were marked significant effects on deactivation, with faster time course. The crystal structure of the herg PAS domain has been obtained (Morais Cabral et al. 1998). The view shown in Fig. 5b includes residue F29 which has previously been shown to lie on a hydrophobic band (Morais Cabral et al. 1998); other LQT2 residues (all affecting deactivation) are situated on the surface of the domain close by. The remaining PAS mutants studied here lie on the reverse face of the domain, not shown in Fig. 5b. Although we did not study here the inactivation properties of the PAS domain mutants, some of these mutations (N33T and R56Q) have been previously

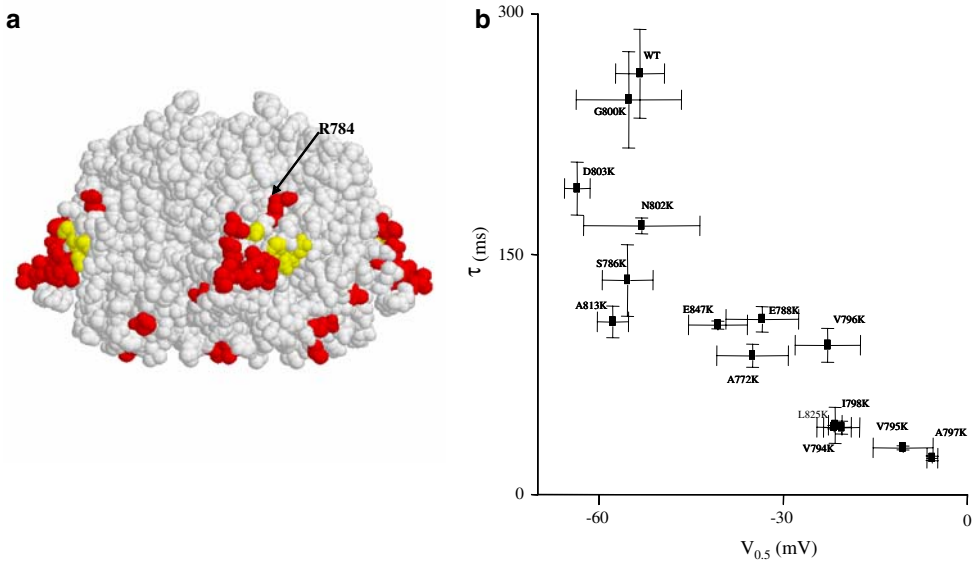


**Fig. 4** Homology model of the herg cNBD tetramer. **a** The residues coloured *red* are those with significant right shift in inactivation as well as significant decrease in time constant of deactivation for lysine mutations as compared with wild type; residues coloured *yellow* did not have significant effect on inactivation. The residue corresponding to LQT2 mutation R784W is also indicated. **b** Using the same data as in Figs. 1 and 3, the value of deactivation time constant, $\tau$, is shown plotted against $V_{0.5}$ for inactivation

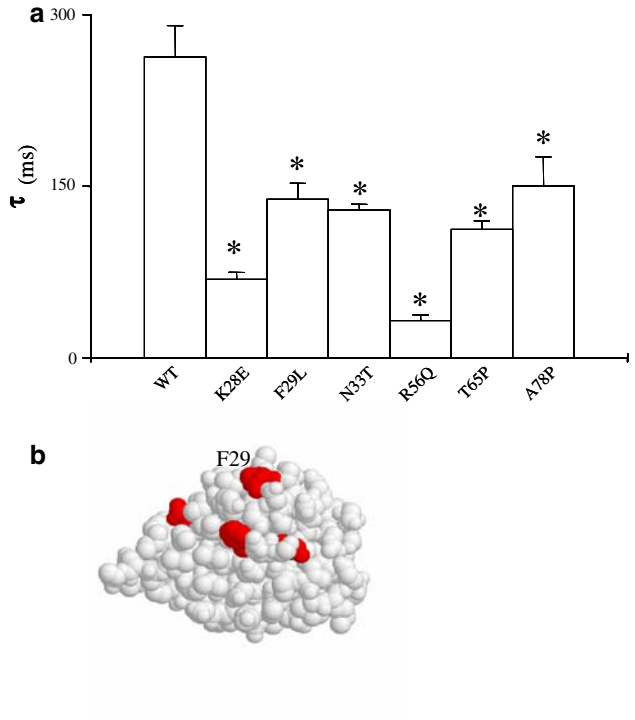


**Fig. 5** Deactivation time course of LQT2 mutants in the PAS domain. **a** The mean time constant for the fast component of deactivation, $\tau$, measured at −70 mV, is shown for the PAS domain mutations indicated ($n$ = 8–22 cells, $^*P < 0.05$). **b** The structure of the herg PAS domain (Morais Cabral et al. 1998) is shown, with residue F29 indicated; LQT2 surface residues visible in this view are indicated in *red* (all affected deactivation time course)

examined and shown to display shifts to the right in inactivation (Chen et al. 1999).

## Discussion

In this study, we have examined the effect of lysine mutations at surface residues of the cNBD. We showed that there is a band of residues on the surface of this domain that affects both deactivation time course and steady-state inactivation (Fig. 4). The band lies in a region with conserved and hydrophobic residues. This suggests that there is a region of functional importance located on the surface of the cNBD which may interact with other parts of the herg channel protein. Thus intracellular elements of the herg channel, in addition to the membrane-spanning region and drug-binding sites on the pore region of the channel, play a key role in regulating channel function.

A similar mutational approach to ours has been carried out on the PAS domain (Morais Cabral et al. 1998), and a patch of hydrophobic residues was identified on the surface of the latter domain which may participate in interactions. In order to compare LQT2 PAS mutations under the same experimental conditions, we have also studied such PAS mutations, showing their contribution to speeding up the rate of deactivation, in agreement with previous work (Chen et al. 1999; Paulussen et al. 2002; Rossenbacker et al. 2005). In particular, LQT2 mutation at residue F29 lies in the hydrophobic patch and was also identified by Morais Cabral et al. (1998) within the band. Thus some of the LQT2 residues at least may affect function via disturbing intracellular interactions within the herg channel protein. Similarly the LQT2 mutation R784W in the cNBD (Yang et al. 2002) lies on the surface of the domain close to the band of residues that we identified on the cNBD (Fig. 4a), and thus may also produce its effect by altering interactions with the herg channel protein.

As lysine mutations may disrupt domain–domain interactions at overlapping hydrophobic regions, the predicted position for the mutated residues provides evidence that the cNBD interacts with other elements of the channel. The precise nature of the intracellular interactions is unknown; so for example the cNBD domain could interact with the PAS domain which may lie at the sides of the cNBD, as suggested may occur for the homologous heag channel (Ju and Wray 2006; Wray 2008). Furthermore, mutations in the N terminus and cytoplasmic S4-S5 linker affect deactivation (Sanguinetti and Xu 1999, Terlau et al. 1997), suggesting interactions with the membrane region. The functional effects of the cNBD domain may involve interactions with other intracellular elements or directly with the membrane-spanning part.

In contrast to the above effects, none of the lysine mutations affected steady-state activation, indicating that the herg cNBD does not play a role in activation of the channel, in contrast to the role of this domain in the HCN channel (Clayton et al. 2004). However, the lack of effect on activation does illustrate that the alteration of the rate of deactivation of the channel is a specific effect of the mutations, rather than a non-specific disruption of the channel's conformation. Indeed, for the heag1 channel, mutations of the cNBD also did not affect steady-state activation, although many alanine mutations affected activation kinetics. Furthermore the band of residues that we have identified in herg by lysine mutations of cNBD residues lies in a corresponding region of the heag1 channel where alanine mutations affected activation kinetics (Wray 2008).

We have found that several of the lysine mutations in the herg cNBD caused large positive shifts in steady-state inactivation. Herg inactivation is characterised by C-type inactivation (Piper et al. 2003; McPate et al. 2005; Torres et al. 2003), which is apparently due to residues located in the extracellular mouth of the pore such as the S5-P region. Therefore the marked effects of the cNBD on inactivation also suggest a crucial role for the cNBD, the mechanism of which is still not understood. It may be that inactivation is a

property involving conformational movement of the channel protein as a whole and not just the extracellular pore region. Deactivation in the herg channel was mainly thought to involve the first 25 or so amino acids of the N terminus (Wang et al. 1998). However, here we have shown that mutations in both the PAS and cNBD domains also have important effects in causing a speeding up of deactivation of the herg channel, so that indeed deactivation may also involve conformational changes of the whole channel (though presumably not the same conformational changes as inactivation). As mentioned above, interactions with the cNBD could be passed on to the rest of the protein via the PAS domains and/or via the intracellular membrane loops such as the S4-S5 linker (Sanguinetti and Xu 1999; Wang et al. 1998).

In summary, using lysine mutations of the cNBD, we have shown that a band of residues on the surface of this domain affect inactivation and deactivation. Such an approach using lysine mutations is useful in identifying likely regions of interaction of the hydrophobic surface of the domain involved in interactions with other parts of the channel protein. One of the LQT2 mutations that we studied (R784W) lies in close proximity to this band of residues on the cNBD, and indeed some other LQT2 mutations on the PAS domain also lie close to a hydrophobic band on the PAS domain.

**Acknowledgments** This work was supported by a project grant to DW from the British Heart Foundation.

## References

Bracey K, Wray D (2006) Inherited disorders of ion channels. In: Voltage-gated ion channels as drug targets. Wiley, New York, pp 381–427

Morais Cabral JH, Lee A, Cohen SL, Chait BT, Li M, Mackinnon R (1998) Crystal structure and functional analysis of the HERG potassium channel N terminus: a eukaryotic PAS domain. Cell 95:649–655. doi:10.1016/S0092-8674(00)81635-9

Chen J, Zou A, Splawski, Keating M, Sanguinetti MC (1999) Long QT syndrome-associated mutations in the Per-Arnt-Sim (PAS) domain of HERG potassium channels accelerate channel deactivation. J Biol Chem 274:10113–10118. doi:10.1074/jbc.274.15.10113

Clayton GM, Silverman WR, Heginbotham L, Morais-Cabral JH (2004) Structural basis of ligand activation in a cyclic nucleotide regulated potassium channel. Cell 119:615–627. doi:10.1016/j.cell.2004.10.030

Ferrer T, Rupp J, Piper DR, Tristani-Firouzi M (2006) The S4-S5 linker directly couples voltage sensor movement to the activation gate in the human ether-a-go-go-related gene (hERG) K+ channel. J Biol Chem 281:12858–12864. doi:10.1074/jbc.M513518200

Finlayson K, Witchel HJ, McCulloch Starkey J (2004) Acquired QT interval prolongation and HERG: implications for drug discovery and development. Eur J Pharmacol 500:129–142. doi:10.1016/j.ejphar.2004.07.019

Ju M, Wray D (2006) Molecular regions responsible for differences in activation between heag channels. Biochem Biophys Res Commun 342:1088–1097. doi:10.1016/j.bbrc.2006.02.062

Kobori A, Sarai N, Shimizu W, Nakamura Y, Murakami Y, Makiyama T, Ohno S, Takenaka K, Ninomiya T, Fujiwara Y, Matsuoka S, Takano M, Noma A, Kita T, Horie M (2004) Additional gene variants reduce effectiveness of beta-blockers in the LQT1 form of long QT syndrome. J Cardiovasc Electrophysiol 15:190–199. doi:10.1046/j.1540-8167.2004.03212.x

Lehmann-Horn F, Jurkat-Rott K (1999) Voltage-gated ion channels and hereditary disease. Physiol Rev 79(4):1317–1372

Li-Smerina Y, Swartza KJ (2001) Helical structure of the COOH terminus of S3 and its contribution to the gating modifier toxin receptor in voltage-gated ion channels. J Gen Physiol 117:205–217. doi:10.1085/jgp.117.3.205

McPate MJ, Duncan RS, Milnes JT, Witchel HJ, Hancox JC (2005) The N588K-HERG $K^+$ channel mutation in the 'short QT syndrome': Mechanism of gain-in-function determined at 37°C. Biochem Biophys Res Commun 334:441–449. doi:10.1016/j.bbrc.2005.06.112

Moss AJ, Zareba W, Kaufman ES, Gartman E, Peterson DR, Benhorin J, Towbin JA, Keating MT, Priori SG, Schwartz PJ, Vincent GM, Robinson JL, Andrews ML, Feng C, Hall WJ, Medina A, Zhang L, Wang Z (2002) Increased risk of arrhythmic events in long-QT syndrome with mutations in the pore region of the human ether-a-go-go–related gene potassium channel. Circulation 105:794–799. doi:10.1161/hc0702.105124

Numaguchi H, Mullins FM, Johnson JP, Johns DC, Po SS, Yang ICH, Tomaselli GF, Balser JR (2000) Probing the interaction between inactivation gating and Dd-sotalol block of HERG. Circ Res 87:1012–1018

Paulussen A, Raes A, Matthijs G, Snyders DJ, Cohen N, Aerssens J (2002) HERG mutation predicts short QT based on channel kinetics but causes long QT by heterotetrameric trafficking deficiency. J Biol Chem 277:48610–48616. doi:10.1074/jbc.M206569200

Piper DR, Varghese A, Sanguinetti MC, Tristani-Firouzi M (2003) Gating currents associated with intramembrane charge displacement in HERG potassium channels. Proc Natl Acad Sci USA 100:10534–10539. doi:10.1073/pnas.1832721100

Rossenbacker T, Mubagwa K, Jongbloed RJ, Vereecke J, Devriendt K, Gewillig M, Carmeliet E, Collen D, Heidbüchel H, Carmeliet P (2005) Novel mutation in the per-arnt-sim Domain of KCNH2 causes a malignant form of long-QT syndrome. Circulation 111:961–968. doi:10.1161/01.CIR.0000156327.35255.D8

Sanguinetti MC, Xu QP (1999) Mutations of the S4-S5 linker alter activation properties of HERG potassium channels expressed in *Xenopus oocytes*. J Physiol 514:667–675. doi:10.1111/j.1469-7793.1999.667ad.x

Sanguinetti MC, Jiang C, Curran ME, Keating MT (1995) A mechanistic link between an inherited and an acquired cardiac arrhythmia. Cell 21 81(2):299–307

Sine SM, Wang HL, Bren N (2002) Lysine scanning mutagenesis delineates structural model of the nicotinic receptor ligand binding domain. J Biol Chem 277:29210–29223. doi:10.1074/jbc.M203396200

Terlau H, Heinemann SH, Stuhmer W, Pongs O, Ludwig J (1997) Amino terminal-dependent gating of the potassium channel rat eag is compensated by a mutation in the S4 segment. J Physiol 502:537–543. doi:10.1111/j.1469-7793.1997.537bj.x

Torres AM, Bansal PS, Sunde M, Clarke CE, Bursill JA, Smith DJ, Bauskin A, Breit SN, Campbell TJ, Alewood PF, Kuchel PW, Vandenberg JI (2003) Structure of the HERG K+ channel S5-P extracellular linker: role of an amphipathic alphahelix in C-type inactivation. J Biol Chem 278:42136–42148. doi:10.1074/jbc.M212824200

Tseng GN (2001) I(Kr): the hERG channel. J Mol Cell Cardiol 33:835–849. doi:10.1006/jmcc.2000.1317

Vandenberg JI, Torres AM, Campbell TJ, Kuchel PW (2004) The hERG K+ channel: progress in understanding the molecular basis

of its unusual gating kinetics. Eur Biophys J 33:89–97. doi:10.1007/s00249-004-0419-y

Wang J, Trudeau MC, Zappia AM, Robertson GA (1998) Regulation of deactivation by an amino terminal domain in human ether-à-go-go-related gene potassium channels. J Gen Physiol 112:637–647. doi:10.1085/jgp.112.5.637

Warmke JW, Ganetzky B (1994) A family of potassium channel genes related to eag in Drosophila and mammals. Proc Natl Acad Sci USA 91:3438–3442. doi:10.1073/pnas.91.8.3438

Wray D (2008) Intracellular regions of potassium channels: Kv2.1 and heag. Eur Biophys J. doi:10.1007/s00249-008-0354-4

Wu P, Wang P (2004) Per-Arnt-Sim domain-dependent association of cAMP-phosphodiesterase 8A1 with I$\kappa$B proteins. Proc Natl Acad Sci USA 101:17634–17639. doi:10.1073/pnas.0407649101

Yang P, Kanki H, Drolet B, Yang T, Wei J, Viswanathan PC, Hohnloser SH, Shimizu W, Schwartz PJ, Stanton M, Murray KT, Norris K, George AL Jr, Roden DM (2002) Allelic variants in long-QT disease genes in patients with drug-associated torsades de pointes. Circulation 105:1943–1948. doi:10.1161/01.CIR.0000014448.19052.4C

Yusaf SP, Wray D, Sivaprasadarao A (1996) Measurement of the movement of the S4 segment during the activation of a voltage-gated potassium channel. Pflugers Arch 433:91–97. doi:10.1007/s004240050253

Zagotta WN, Olivier NB, Black KD, Young EC, Olson R, Gouaux E (2003) Structural basis for modulation and agonist specificity of HCN pacemaker channels. Nature 425:200–205. doi:10.1038/nature01922

Zhulin IB, Taylor BL, Dixon R (1997) PAS domain S-boxes in archaea, bacteria and sensors for oxygen and redox. Trends Biochem Sci 22:331–333. doi:10.1016/S0968-0004(97)01110-9